Published in final edited form as:
*Cortex*. 2010 February ; 46(2): 206–216. doi:10.1016/j.cortex.2009.03.008.

# Developmental changes in cerebral white matter microstructure in a disorder of lysosomal storage

**Sunita Bava**[1,2], **Rebecca J. Theilmann**[2], **Miriam Sach**[1], **Susanne J. May**[1,3], **Lawrence R. Frank**[2,4], **John R. Hesselink**[2], **Duc Vu**[1], and **Doris A. Trauner**[1,5,*]

[1]Department of Neurosciences, University of California, San Diego

[2]Department of Radiology, University of California, San Diego

[3]Department of Family and Preventive Medicine, University of California, San Diego

[4]VA San Diego Healthcare System

[5]Department of Pediatrics, University of California, San Diego

## Abstract

The goal of this work was to study white matter integrity in children with cystinosis, a rare lysosomal storage disorder resulting in cystine accumulation in peripheral and central nervous system tissue. Based on previous reports of cystine crystal formation in myelin precursors as well as evidence for specific cognitive deficits in visuospatial functioning, diffusion tensor imaging (DTI) was applied to 24 children with cystinosis (age 3–7 years) and to 24 typically developing age-matched controls. Scalar diffusion indices, fractional anisotropy (FA) and mean diffusivity (MD), were examined in manually-defined regions of interest within the parietal and inferior temporal lobes. Diffusion indices were correlated with performance on measures of visuospatial cognition and with white blood cell cystine levels. Bilaterally decreased FA and increased MD were evident in the inferior and superior parietal lobules in children with cystinosis, with comparable FA and MD to controls in inferior temporal white matter, and implicate a dissociation of the dorsal and ventral visual pathways. In older cystinosis children (age > 5), diminutions in visuospatial performance were associated with reduced FA in the right inferior parietal lobule. In addition, increased MD was found in the presence of high cystine levels in all children with cystinosis. This study provides new information that the average diffusion properties in children with cystinosis deviate from typically developing children. Findings suggest the presence of early microstructural white matter changes in addition to a secondary effect of cystine accumulation. These alterations may impact the development of efficient fiber networks important for visuospatial cognition.

### Keywords

Cystinosis; Lysosomal storage disorder; DTI; Children; Visuospatial



*Address correspondence to: Doris Trauner, M.D. 9500 Gilman Drive, MC 0935 La Jolla, CA 92093-0935 Phone: (858) 822-6700 Fax: (858) 822-6707 dtrauner@ucsd.edu.

## 1. Introduction

Infantile nephropathic cystinosis is a lysosomal storage disorder that is autosomal recessive in inheritance (Gahl et al., 2002). The genetic defect is one of cystine transport, wherein the accumulation of cystine within lysosomes results in the formation of crystals in multiple organs including the brain (Gahl, 1986). Although the mechanism of tissue damage is unclear, renal tubular dysfunction, growth retardation, hypothyroidism, progressive myopathy and central nervous system deterioration are among the resultant chronic effects (Charnas et al., 1994; Ehrich et al., 1979; Fink et al., 1989; Gahl et al., 1988).

Despite newer cystine-depleting treatments, subtle neurological deficits remain and are apparent early in development (Cochat et al., 1986; Ross et al., 1982; Trauner et al., 2007). Among these, neurocognitive weaknesses are a prevalent concern and are predominant in the visuospatial domain, accompanied by impairments in arithmetic and tactile recognition (Ballantyne et al., 1997; Colah and Trauner, 1997; Trauner et al., 1988). Deficits in the visual domain are isolated to the spatial component of visual function, as visual-perceptual functions are largely intact (Ballantyne and Trauner, 2000). The development of visuospatial functions appears to be impacted early in life, with deficits observed in children at least as young as 3 years of age (Trauner et al., 2007).

Although the neuropathology underlying this cognitive profile is unknown, postmortem studies show alterations throughout the brain parenchyma in cystinosis. Most distinctive and specific to this condition is that of cystine crystal deposition (Jonas et al., 1987; Levine and Paparo, 1982), which is found in several cell types, but most commonly within pericytes, parenchymal cells of white matter (WM) and oligodendrocytes (Vogel et al., 1990). Ventricular dilatation consistent with cortical and WM atrophy is evident in adults (Cochat et al., 1986; Fink et al., 1989; Nichols et al., 1990), though the onset and pathogenesis of these processes is unclear.

To examine the early effects of this genetic disorder on WM development, we employed diffusion tensor imaging (DTI) to assess the integrity of component regions within the visual processing streams. DTI is sensitive to the random motions, or diffusion, of water molecules in neural tissue. Through manipulation of diffusion sensitizing gradients along different directions, one can reconstruct the directional dependence of diffusion and, from this, infer the structural characteristics of the local tissue environment (Stejskal and Tanner, 1965). Two standard diffusion-sensitive scalar measures can be derived from DTI that provide information on underlying WM structure: the mean diffusivity (MD), a measurement of the overall magnitude of diffusional motion within a given voxel, and the fractional anisotropy (FA), a measurement of the directional variance of diffusional motion (Basser and Pierpaoli, 1998; Moritani et al., 2004).

Considering that the profile of impaired spatial and spared perceptual processing in children with cystinosis parallels the well known dissociation between the dorsal and ventral processing streams (Ungerleider and Mishkin, 1982), we predicted that children with cystinosis would demonstrate lower FA in dorsal pathway regions, but similar FA to controls in ventral regions. This would suggest attenuated white matter quality in spatial analytic and action-relevant visuospatial processing regions in the context of preserved white matter integrity in perceptual processing regions specialized for object identification and discrimination (DeYoe and Van Essen, 1988; Ungerleider and Haxby, 1994). Secondly, we hypothesized that the severity of the visuospatial deficit in children with cystinosis would be negatively correlated with FA in dorsal pathway regions, as consistent with recent findings linking increased anisotropic diffusion to efficient cognitive performance, (Fryer et al., 2008; Schmithorst et al., 2005). Although largely unexplored as a marker of disease

load, we predicted that white blood cell cystine level near the time of testing would be negatively correlated with visuospatial function and FA in parietal regions.

## 2. Methods

### 2.1 Participants

Forty-eight children ranging in age from 3 through 7 years (mean age, 5.5 ± 1.3 years) participated in the current study. Twenty-four of these children (10 male, 14 female) were diagnosed with infantile nephropathic cystinosis. A control group consisting of 24 typically developing children (12 male, 12 female) were individually matched to the cystinosis children on the basis of age (± 6 months) and socioeconomic status. The diagnosis of cystinosis was confirmed based on genetic testing or elevated leukocyte cystine levels (Smith et al., 1987; Smolin et al., 1987) in addition to clinical history. All cystinosis participants were screened to ensure that they were not experiencing renal failure at the time of testing, that they were euthyroid, had adequate vision for testing, and were free from other neurological and psychiatric conditions. In addition, we verified that no cystinosis children in our study had a history of pulmonary dysfunction or diabetes mellitus, due to the potential impact of these conditions on neurobehavioral functioning. Cystinosis children were recruited through the National Cystinosis Foundation, the Cystinosis Research Network, and the Cystinosis Research Foundation, all of which maintain close contact with many cystinosis families. Control participants were screened with a comprehensive family and medical history questionnaire and the age-appropriate Wechsler Intelligence Scale (Wechsler, 1991; Wechsler, 1989). Exclusionary criteria were: history of neurodevelopmental or medical disorder including brain damage from closed head trauma, hypoxic-ischemic encephalopathy, meningitis or encephalitis, or acute systemic illness that might adversely affect cognitive function; significant alcohol or illicit drug exposure in utero; learning disability; intellectual (Wechsler Intelligence Quotient (IQ) < 85), behavioral, or psychiatric problems; and clinically abnormal brain anatomy based on neuroradiological review of structural MRIs collected as part of this study. Informed consent was obtained from participants' parents/legal guardians in accordance with University of California, San Diego Institutional Review Board procedures.

### 2.2 MR acquisition

Prior to imaging, participants were administered diphenhydramine or clonidine orally to facilitate relaxing and/or falling asleep during scanning. A physician or nurse practitioner presided over medication administration. After lying in the scanner, foam pads were placed around the head to minimize head motion. Participants were imaged in a 1.5T General Electric Clinical MRI magnet (EXCITE HD). Diffusion weighted imaging consisted of a single-shot dual spin echo excitation with b-values of 0 and 2,000 s/mm$^2$ (TR = 105 ms, TE = 82.2 ms, field of view (FOV) = 24 cm, flip angle = 90°, matrix = 128 × 128 interpolated to 256 × 256, 3.8 mm contiguous slices). The diffusion sampling scheme is the simple model method of Basser and Peripaoli (1998). It assumes Gaussian diffusion and can be described by a symmetric 3×3 diffusion tensor. Therefore, it requires six different diffusion weighting directions and a seventh normalizing image with a b-value of 0 s/mm$^2$ and a gradient coordinate system (*x,y,z*): (0,1,1); (0,1,−1); (1,0,1); (1,0,−1); (1,1,0); and (1,−1,0). Two series were collected to increase signal-to-noise ratio and were externally averaged. High resolution T1-weighted sagittal images acquired using a spoiled gradient echo (SPGR) sequence (TR = 20 ms, TE = 4 ms, FOV = 25 cm, flip angle = 90°, matrix = 128 × 128 interpolated to 256 × 256, 1.3 mm contiguous slices), covering the entire cerebral volume, provided an anatomical reference for manual definition of regions of interest (ROIs). All MRI scans received a clinical reading by a neuroradiologist (JRH) blinded to subject status.

### 2.3 Image processing and DTI Quantification

Prior to data analysis, images were assessed for sufficient quality. Those data deemed invalid due to technical problems or artifacts were excluded from the study. Four participants (2 cystinosis, 2 controls) were excluded due to severe motion artifacts. Two participants (1 cystinosis, 1 control) were excluded due to susceptibility artifacts.

Following data inspection, each diffusion-weighted dataset was aligned to the first volume to correct for motion occurring between the two image sets in AMIRA 3.1 (Mercury Computer Systems Inc., Chelmsford, MS, USA) using a rigid body only registration with no rotations. Once completed, the two image sets were averaged to improve signal-to-noise ratio and registered using a similar rigid body transformation to the B0 image to minimize eddy current distortions. Pre-processed images were then subjected to tensor decomposition to derive scalar diffusion indices, FA and MD (Le Bihan et al., 2001). This computation was performed in native coordinate space using Analysis of Functional NeuroImages' (Cox, 1996) diffusion plugin routine, *3dDWItoDT* (Cox and Glen, 2006), which provides a non-linear positive definite estimation of the diffusion tensor. Values of FA and MD were then calculated on a voxel-by-voxel basis.

The following procedures were implemented in SPM2 (Statistical Parametric Mapping, Welcome Department of Imaging Neuroscience, University College London). To ensure inter-individual anatomical alignment, the T1-weighted anatomical images of all subjects were aligned to the anterior and posterior commissure (ACPC). FA and MD maps were then coregistered to the anatomical images using a mutual information method (Ashburner et al., 1997). Segmentation of the anatomical images into three separate tissue classes representing gray matter (GM), WM, and cerebrospinal fluid (CSF) was performed using a combined anatomical a priori knowledge and pixel intensity approach, resulting in tissue probability maps (Ashburner and Friston, 1997). The segmented WM images served as masks from which FA and MD values were extracted (Barnea-Goraly et al., 2005; Schmithorst et al., 2002) using AMIRA.

### 2.4 Region of Interest Analysis

Regions were defined in AMIRA by manually tracing on each ACPC-aligned high resolution anatomical image. Manual definition was implemented to minimize the confound of including adjacent structures (Schneider et al., 2004; Snook et al., 2005). This method confers an advantage over faster but more simplistic techniques of placing geometric shapes over a certain area or interpolating over the brain volume. Based on previous findings of the probable anatomical correlates of visuospatial function (Just et al., 2001; Klingberg et al., 2002; Oliver and Thompson-Schill, 2003; Rao et al., 2003; Thomas et al., 1999), selected ROIs including the left and right inferior parietal lobule (LIPL; RIPL), the left and right superior parietal lobule (LSPL; RSPL), and for purposes of demonstrating a dissociation, the left and right inferior temporal gyrus (LITG; RITG) were examined (Pins et al., 2004; Schmithorst et al., 2007b; Shen et al., 1999).

Each region's limiting sulci, gyri and anatomical landmarks were located by viewing the anatomical images in three orthogonal planes. Use of a surface rendering algorithm (AMIRA Voltex) provided a three-dimensional view of the relevant structures, allowing rotation around x, y, and z axes to achieve the best possible visualization of each region. Outlines were drawn around relevant brain regions and filled in using AMIRA routines and manual editing.

Standardized rules were generated for delineating each ROI. The parietal lobe was traced first (Figure 1a) before parcellation into superior and inferior lobules (Crespo-Facorro et al., 2000; Kates et al., 1999). The parietal lobe was traced primarily in the sagittal plane,

beginning off center from the midline and progressing laterally. The fronto-parietal border of the parietal lobe was delineated by the central sulcus and the parieto-occipital fissure marked the posterior border. As the corpus callosum disappears, the lobe was traced as all matter above the lateral ventricle extending to the superior aspect of the hippocampus. Following definition of the parietal lobe, the postcentral gyrus was extracted and the remaining region was subdivided into the IPL and SPL. The anatomical boundaries of the IPL consisted of the post-central sulcus as the anterior border, the intraparietal sulcus as the superior border, and the lateral fissure as the anterior inferior border. The SPL, which emerges medial to the supramarginal and angular gyrus is bounded anteriorly by the post-central sulcus and posteriorly by the parieto-occipital fissure. The ITG was located and drawn on both the lateral and ventral surfaces of the hemisphere using the inferior temporal sulcus and occipito-temporal sulcus as boundaries (Kim et al., 2000). Tracing of the ITG terminated medially as the insula fused with the superior temporal gyrus. Region definition was performed in the right and left hemisphere.

The interrater reliability of the ROI-defining procedures was obtained for each region between two trained staff members. Reliability for each ROI was evaluated in three randomly selected cases assessed by the two raters. Intraclass correlation coefficients were 0.95 for the LSPL, 0.96 for the RSPL, 0.95 for the LIPL, 0.97 for the RIPL, 0.96 for the LITG, and 0.96 for the RITG. Following ROI definition, ROI and segmented WM masks were applied to FA and MD maps (Figure 1a–d depicts this process) for statistical comparison using AMIRA.

### 2.5 Visuospatial Assessment

Two measures of visuospatial cognition, the Spatial Relations test of the Woodcock-Johnson Psycho-Educational Battery Third Edition (WJ-III)(McGrew and Woodcock, 1985) and the Copy and Coordination component of the Beery-Buktenica Developmental Test of Visual Motor Integration, 5th Edition (VMI) (Beery et al., 2004), were administered to each participant to examine the relationship between diffusion parameters and behavioral performance. These measures have demonstrated sensitivity to the visuospatial deficits in young children with cystinosis (Trauner et al., 2007) and were chosen accordingly. The Spatial Relations test requires participants to visually select from a series of shapes, the component parts required to make a whole. Mental rotation of each element is required to form a correct whole and shapes become increasingly more abstract and complex as the test progresses. The VMI assesses the integration of visual and motor abilities. The Copy and Coordination measure consists of 27 geometric forms presented in developmental sequence. Participants are asked to copy each form in successive order. All protocols are scored by two independent raters to ensure interrater reliability equivalent to at least 95% overall agreement. Raw scores from both measures are standardized for age with a mean of 100 (SD = 15).

Participants were also administered either the Wechsler Preschool and Primary Scale of Intelligence-Revised (WPPSI-R) (Wechsler, 1989) or the Wechsler Intelligence Scale for Children-III (WISC-III) (Wechsler, 1991), depending on age, in order to covary for differences in intellectual functioning.

### 2.6 Cystine Levels

Cystinosis participants' white blood cell cystine levels were obtained from medical records. The appropriate Health Insurance Portability and Accountability Act (HIPAA) research authorization was obtained from the parent or legal guardian prior to accessing cystine lab panels. White blood cell cystine levels were analyzed in traditional units (nmol of half-cystine per milligram of protein). Correlation analysis of white blood cystine level with

diffusion maps and visuospatial functioning was performed if cystine measurements occurred within two months of participation in the study. Lifetime cystine levels were analyzed if two measurements at minimum were collected during each year of life. This criterion was adopted to account for possible fluctuations in cystine levels that can occur within a given year of life. Requiring that at least two measurements occurred during each year of life, provided an estimate of cystine level that could account for variance across timepoints.

### 2.7 Statistical Analysis

Prior to analysis, independent and dependent variables were examined for normality using a test for skewness and kurtosis. Although cognitive measures were normally distributed, FA, MD and cystine level were found to deviate from normality. Results of Levene's test for homogeneity of error variances were satisfactory ($p > .05$). Statistical comparisons were performed in a parametric framework when modeling multiple covariates, but univariate analyses were replicated using nonparametric methods, where appropriate, to ensure robustness of our findings.

A multivariate analysis of variance (MANOVA) tested for group differences in FA and MD, each separately, over four regions of the parietal lobe and two regions of the temporal lobe. As brain structure and diffusion properties change with age and differ between males and females (Schmithorst et al., 2007a), we examined the effect of potential covariates including age and sex on FA and MD. Spearman correlations assessed the relationship between visuospatial performance, cystine level, and FA and MD in parietal regions.

Analyses across multiple regions employed Hochberg correction for multiple comparisons (maintaining $\alpha_{FW} = .05$), with FA and MD analyses constituting separate families of comparisons. P-values reported are adjusted for the Hochberg correction. Cook's distance statistic was used to identify potentially influential observations and Levene's test assessed the homogeneity of error variance between groups.

A concern in the design and analytic approach of this study was the issue of power. Due to the rare nature of cystinosis the sample size was necessarily small, thus limiting the power of the study. Secondly, to ensure Type I error control, adjustments were made for multiple comparisons on a family-wise basis. As a result, the current study had limited power to detect very small or medium effects. It is important to consider that statistically significant findings ($p < .05$) reported here, represent notably large and clinically meaningful effect sizes.

## 3. Results

Examination of our data distribution revealed one outlier in the cystinosis group with extremely low FA in parietal regions. Influence statistics including Cook's distance (critical value = 13.79, maximum sample value = 9.31) did not identify this case or any others as multivariate outliers in their respective groups. Moreover, analyses were repeated while omitting this participant and findings remained unchanged.

### 3.1 Behavioral Performance

A multivariate analysis of covariance was performed on two measures of visuospatial functioning and two measures of intellectual functioning (WJ-III Spatial Relations Subtest, Beery VMI, Wechsler Verbal IQ, and Wechsler Performance IQ) to compare performance between the cystinosis and control groups, with age as a covariate. There was a significant main effect of group ($F_{(1,46)} = 36.87$, $p < .0001$), such that the cystinosis group performed

worse than controls overall (see Table 1). Comparison of overall profiles did not indicate significant deviations from parallelism.

### 3.2 Clinical MRI Readings

Three cystinosis children showed evidence of mild cortical atrophy, one showed mild central atrophy (ventriculomegaly), and four demonstrated mild to moderate cortical and central atrophy. No gray or white matter lesions were noted by the neuroradiologist.

### 3.3 Fractional Anisotropy and Mean Diffusivity

Potential covariates including age and sex were examined in relation to diffusion parameters. Following correction for multiple comparisons, Spearman correlations indicated a positive relationship between age and FA in the LIPL ($r = .45$, $p = .03$), LSPL ($r = .46$, $p = .02$), RIPL ($r = .43$, $p = .03$), and RSPL ($r = .56$, $p = .005$) for the cystinosis group only (see Figure 2). Significant negative correlations between age and MD were evident in the LIPL ($r = -.49$, $p = .01$), RIPL ($r = -.61$, $p = .001$), and RSPL ($r = -.46$, $p = .02$) in the cystinosis group and in the LIPL ($r = -.41$, $p = .04$) for controls. Given the interaction between age and group, age was included as an independent variable in further ROI analyses. No sex differences in FA or MD were apparent.

Within-group comparisons revealed symmetrical values of FA and MD across parietal regions in control children. In the cystinosis group, FA was significantly lower in the RIPL as compared to the homologous region in the left hemisphere ($t_{(23)} = 2.60$, $p = .02$). Consistent with our hypothesis, between-group comparisons using MANOVA indicated significantly decreased FA in the bilateral SPL and RIPL of cystinosis children relative to controls (see Table 2). This finding occurred in the context of non-significant differences in FA in temporal regions. Interestingly, alterations in FA were more pronounced for younger cystinosis children (age ≤ 5.50, $n = 11$) in all four parietal regions (LIPL: p = .01; LSPL: p = .004; RIPL: p = .02; RSPL: p = .002), whereas older children with cystinosis (age > 5.50, $n = 13$) demonstrated mean FA values approximating those of controls ($p = .54$ to .98) (see Figure 2).

As shown in Table 2, analysis of MD revealed significantly increased diffusivity in bilateral SPL in the cystinosis group as compared to controls. In concordance with FA findings, group differences in MD were not evident in temporal regions. Nonparametric statistics using the Mann-Whitney U Test replicated all between-group findings, though significantly increased MD in the cystinosis group was additionally evident in the LIPL ($z = -2.17$, $p = .03$) and RIPL ($z = -2.0$, $p = .05$).

Subsidiary analyses were performed on a subgroup of cystinosis participants with normal radiological brain MRI scans ($n = 12$) to address the potential confound of cortical and/or central atrophy as contributing to differences between groups. The results of these analyses replicated those previously described. In particular, even after selecting cystinosis participants without evidence of brain abnormality on MRI, they continued to show reduced FA in parietal regions as compared to age-matched controls.

### 3.4 Correlation with Visuospatial Performance and Cystine Levels

Correlation of FA and MD in parietal regions with visuospatial functioning did not reveal significant findings for either group. Considering the significant relationship between age and diffusion parameters found only in the cystinosis group, we examined whether age moderated correlations between FA or MD and visuospatial functioning. Analysis of school-age cystinosis participants (age > 5.50, $n = 13$) revealed a positive relationship between FA in the RIPL and performance on the Beery VMI ($r = .74$; $p = .004$) (see Figure 3), with no

such relationships evident in temporal ROIs. No significant correlations emerged between diffusion parameters and the Spatial Relations subtest or between MD and Beery VMI performance.

Examination of cystine levels and diffusion parameters ($n = 17$) indicated a positive relationship between white blood cell cystine level at the time of testing and RSPL MD ($r = .50$, $p = .04$), and a similar trend in relation to RIPL MD ($r = .46$, $p = .05$). Analysis of school-age cystinosis participants (age > 5.50, $n = 10$), extended findings from the total group. Specifically, positive correlations between cystine level at the time of testing and LIPL MD ($r = .93$, $p = .001$), LSPL MD ($r = .91$, $p = .002$), and RIPL MD ($r = .86$, $p = .007$) were evident. A trend toward a negative relationship between cystine level and RSPL FA was also noted ($r = -.69$, $p = .06$). Additionally, greater variance of cystine levels over one's lifetime was associated with decreased PIQ ($r = -.72$, $p = .04$). Results of analyses repeated to evaluate such relationships in temporal regions, revealed no significant findings.

## 4. Discussion

This is the first study to investigate WM microstructure in children with a disorder of lysosomal storage. Consistent with our hypothesis, children with cystinosis evidenced diminutions in mean FA and corresponding elevation in MD in component areas of the dorsal visual pathway. These changes occurred in the absence of alterations in the inferior temporal area, a predominant region constituting the ventral visual pathway. Bilateral decrements in FA in children with cystinosis appear consistent with the finding that young children require both hemispheres to process visuospatial tasks (Stiles, 2000). Together, these findings suggest that selective changes in cerebral WM are evident in cystinosis and are present early on in development. In addition to early changes, a secondary effect of cystine accumulation on WM maturation and visuospatial functioning is implicated.

### 4.1 Age-related differences in diffusion anisotropy

A central question in characterizing the observed neurological deficits in cystinosis is whether the genetic deletion causes early structural alterations or whether progressive disease processes result in compromise of structure over time. Though this is best investigated with a longitudinal design, the present findings provide some insight regarding neurodevelopmental processes in this condition. Our study demonstrated significant positive correlations between age and diffusion parameters in children with cystinosis, whereas control children exhibited a relatively flat profile across the 3–7 year age range studied. The latter finding is consistent with previous work describing MD and FA over the developmental period. Diffusion indices measured in multiple cerebral regions including the caudate, thalamus, corpus callosum, internal capsule, and frontal and periventricular WM show a rapid increase in FA and decrease in MD during the first 2 years of life. Following this steep pattern, is a slower process of change on through adolescence (Mukherjee et al., 2001; Mukherjee et al., 2002). The slope of FA from 2 to 18 years of age is modest in magnitude particularly for regions subserving higher cognitive functions such as fronto-parietal WM, in which neurodevelopment is relatively more protracted (Schmithorst et al., 2002).

Children with cystinosis show a departure from this developmental pattern. Examination of age-related changes in FA revealed a notable developmental lag at young ages in cystinosis children as compared to typically developing controls. While cystinosis children appear to catch-up by the age of 5.5 years, as reflected in comparable FA to control children, they continue to demonstrate cognitive deficits. This finding is particularly striking as it suggests that the structure of the fiber networks may be inefficiently laid down early in development. Aberrations in the core framework may result in persistent cognitive deficits that cannot be

overcome with maturation. Moreover, initial changes in myelin precursors or cellular components may result in consistently altered WM maturation.

### 4.2 Clinical correlates of FA and MD

The functional implications of WM changes in cystinosis appear to be prominent for school-aged children with cystinosis (>5.5 years), where FA was found to correlate with performance on a task of visual-motor integration. Although mean FA in school-age children with cystinosis begins to approximate that of controls, the nature of fiber organization and connectivity may be qualitatively different, and thus lead to disparate visuospatial cognitive abilities. Given that brain regions involved in spatial analytic processing become more specialized over the course of development, particularly from 6–12 years of age (Akshoomoff and Stiles, 1995), the relationship between FA and performance on visuospatial tasks may not be entirely discernable in younger children with cystinosis (< 5 years).

To explore potential mechanisms of WM pathogenesis in the visual processing streams, a tertiary component of our study focused on white blood cell cystine, a biological marker in cystinosis. High white blood cell cystine levels reflect increased cystine accumulation, which interferes with cellular structure and function (Feksa et al., 2004; Gahl, 1986). The relationship between white blood cell cystine and brain cystine levels is unclear; however, the present findings suggest a potentially important link. Regardless of age, white blood cell cystine level was associated with increased MD in the right SPL with a similar trend evident in the IPL. Although cystine accumulation and resultant crystal formation would be expected to hinder diffusion, it appears that degradation of existing WM tracts or delayed WM development may be a consequence instead. The latter possibility is congruent with the developmental lag in FA observed at very young ages and suggests an early impact of cystine on CNS structure.

Older cystinosis children (> 5 years) demonstrated stronger associations between cystine level and MD in bilateral parietal regions, suggesting that in addition to an initial disruption in WM maturation early in development, there may be a secondary progressive effect of cystine accumulation on WM organization and connectivity. Of note, we begin to see the effect of increased cystine on FA in the older cystinosis group, where we observed a trend toward a negative relationship between cystine level and FA in the RIPL. Although only speculative, this trend may presage regressive processes in the adolescent period. Indeed, in their study of visuomotor integration in children with cystinosis (4 – 16 years of age), (Scarvie et al., 1996) showed that with advancing age, children with cystinosis fell further behind their typically developing peers. Animal models also implicate a progression in cognitive impairment with age that corresponds to an elevation in cystine levels (Maurice et al., 2007).

Although cystine level was not systematically related to visuospatial performance, increased variation in cystine levels over time corresponded to decrements in PIQ (in children > 5 years of age). As alluded to above, structural networks which may be inefficiently laid down at the onset, may also be increasingly vulnerable to fluctuations in cystine. The current findings suggest that white blood cell cystine levels over the course of development may be an important factor in the neuropathogenesis of cystinosis.

### 4.3 Diffusion indices and implications for neuropathogenesis

Alterations in both FA and MD in children with cystinosis could reflect a number of aberrant neurodevelopmental processes. It is possible that anisotropic changes are present early in development, emerging from aberrations in cellular components and membranous

organelles that are directly related to the causative nephropathic cystinosis gene, *CTNS* (Kleta and Gahl, 2004). It is also possible that intracellular cystine crystal formation may simulate cytotoxic edema, as occurs in glial cells, axons, and myelin sheaths. As a result, the accumulation of cystine in the oligodendroglial lysosomes could lead to cell degeneration (Gieselmann et al., 1994; Kessler et al., 2007; van der Knaap et al., 1999). An additional consideration is that an interaction of these processes is at work. Initial cellular and membrane damage set in place at an early point in development may instigate a cascade of events eventually resulting in loss of fiber integrity and hypofunctional cortical networks.

### 4.4 Limitations

Several limitations to the current study must be addressed in future research. Our sample size, while substantial given the rare nature of cystinosis, precluded more extensive analysis of relationships between demographic, neurobiological, and cognitive variables including statistical evaluation of an age by group interaction. The conservative approach of adjusting for multiple comparisons further reduces the statistical power.

Our methods were also limited with regard to our diffusion protocol and processing techniques. In particular, we utilized a 6 direction diffusion model primarily to provide an acceptable scan time for our young participants. This model is insufficient for voxels containing multiple-fiber orientations and can lead to error in estimating diffusion parameters (Frank, 2001; Pierpaoli et al., 1996). High angular resolution techniques should be considered in future work to more accurately model regions of complex fiber distributions and characterize local diffusion.

### 4.5 Future Directions and Conclusion

Longitudinal examination of children in the current study would permit a more comprehensive assessment of the relationship between early changes in brain parenchyma and progressive processes in cystinosis. Brain systems that mediate visuospatial function undergo critical change, particularly in early adolescence, when patterns of functional activation begin to resemble that of adults. Examination of this period of development may provide insight into the progression of WM compromise and related cognitive changes in cystinosis.

Although our study addresses important hypotheses for understanding the neuropathophysiology of cystinosis, the relationship between DTI measures and specific changes to the WM structure are still unclear. Changes in FA may be caused by any combination of factors related to myelination, axonal diameter, fiber density, and coherence. Histological studies may be necessary to identify specific changes to tissue architecture and integrity in cystinosis.

In conclusion, this study provides new evidence that the average DTI properties in children with cystinosis deviate from typically developing children. These differences are evident in parietal regions and appear to vary over the early developmental period, where a developmental lag in WM maturation is implicated. Our findings further suggest that early microstructural changes may impact the development of efficient fiber networks within the dorsal processing stream and result in cognitive skill deficits. In addition, ongoing neurobiological processes in cystinosis may constitute a secondary factor impacting overall behavioral outcome. The present findings are also of clinical significance as they demonstrate early alterations in WM maturation that may result in subtle, but persistent cognitive deficits. Given the critical role of experience in cognitive development and skill acquisition, early intervention in the form of visuospatial skill training may result in greater adjustment to initial disruptions in this system.

## Acknowledgments

This research was supported by the NINDS R01 NS04135. We extend our warmest thanks to the cystinosis children and their families whose participation was vital to the completion of this research. We also express appreciation to Dr. Amy Spilkin, Ms. Jenny Williams, Ms. Lynne Babchuck and the UCSD Pediatric Neurology Research Group for their support of this study and to Drs. Natacha Akshoomoff, Georg Matt, Sarah Mattson, and Susan Tapert for their guidance and suggestions.

## 6. References

Akshoomoff N, Stiles J. Developmental trends in visuospatial analysis and planning: I. Copying a complex figure. Neuropsychology. 1995; 9:364–377.

Ashburner J, Friston KJ. Multimodal image coregistration and partitioning- a unified framework. Neuroimage. 1997; 6:209–217. [PubMed: 9344825]

Ashburner J, Neelin P, Collins DL, Evans A, Friston K. Incorporating prior knowledge into image registration. Neuroimage. 1997; 6:344–352. [PubMed: 9417976]

Ballantyne AO, Scarvie KM, Trauner DA. Academic achievement in individuals with infantile nephropathic cystinosis. Am Journal of Medical Genetics. 1997; 74:157–161.

Ballantyne AO, Trauner DA. Neurobehavioral consequences of a genetic metabolic disorder: visual processing deficits in infantile nephropathic cystinosis. Neuropsychiatry, Neuropsychology and Behavioral Neurology. 2000; 13:254–263.

Barnea-Goraly N, Menon V, Eckert M, Tamm L, Bammer R, Karchemskiy A, Dant CC, Reiss AL. White matter development during childhood and adolescence: a cross-sectional diffusion tensor imaging study. Cerebral Cortex. 2005; 15:1848–1854. [PubMed: 15758200]

Basser PJ, Pierpaoli C. A simplified method to measure the diffusion tensor from seven MR images. Magnetic Resonance in Medicine. 1998; 39:928–934. [PubMed: 9621916]

Beery, KE.; Buktenica, NA.; Beery, NA. Developmental Test of Visual Motor Integration (VMI). 5th Edition. Western Psychological Services; Los Angeles: 2004.

Charnas LR, Luciano CA, Dalakas M, Gilliatt RW, Bernardini I, Ishak K, Cwik VA, Fraker D, Brushart TA, Gahl WA. Distal vacuolar myopathy in nephropathic cystinosis. Annals of Neurology. 1994; 35:181–188. [PubMed: 8109899]

Cochat P, Drachman R, Gagnadoux MF, Pariente D, Broyer M. Cerebral atrophy and nephropathic cystinosis. Archives of Disease in Childhood. 1986; 61:401–403. [PubMed: 3707194]

Colah S, Trauner DA. Tactile recognition in infantile nephropathic cystinosis. Developmental Medicine & Child Neurology. 1997; 39:409–413. [PubMed: 9233367]

Cox R. Software for analysis and visualization of functional magnetic resonance neuroimages. Computers and Biomedical Research. 1996; 29:162–173. [PubMed: 8812068]

Cox, R.; Glen, D. Efficient, Robust, Nonlinear, and Guaranteed Positive Definite Diffusion Tensor Estimation. Proceedings of the International Society for Magnetic Resonance in Medicine, 14th Scientific Meeting; 2006.

Crespo-Facorro B, Kim J, Andreasen NC, Spinks R, O'Leary DS, Bockholt HJ, Harris G, Magnotta VA. Cerebral cortex: a topographic segmentation method using magnetic resonance imaging. Psychiatry Research. 2000; 100:97–126. [PubMed: 11114495]

DeYoe EA, Van Essen DC. Concurrent processing streams in monkey visual cortex. Trends in Neuroscience. 1988; 11:219–226.

Ehrich JH, Stoeppler L, Offner G, Brodehl J. Evidence for cerebral involvement in nephropathic cystinosis. Neuropadiatrie. 1979; 10:128–137. [PubMed: 582846]

Feksa LR, Cornelio A, Dutra-Filho CS, De Souza Wyse AT, Wajner M, Wannmacher CM. Inhibition of pyruvate kinase activity by cystine in brain cortex of rats. Brain Research. 2004; 1012:93–100. [PubMed: 15158165]

Fink JK, Brouwers P, Barton N, Malekzadeh MH, Sato S, Hill S, Cohen WE, Fivush B, Gahl WA. Neurologic complications in long-standing nephropathic cystinosis. Archives of Neurology. 1989; 46:543–548. [PubMed: 2712751]

Frank LR. Anisotropy in high angular resolution diffusion-weighted MRI. Magnetic Resonance in Medicine. 2001; 45:935–939. [PubMed: 11378869]

Fryer SL, Frank LR, Spadoni AD, Theilmann RJ, Nagel BJ, Schweinsburg AD, Tapert SF. Microstructural integrity of the corpus callosum linked with neuropsychological performance in adolescents. Brain and Cognition. 2008

Gahl WA. Cystinosis coming of age. Advances in Pediatrics. 1986; 33:95–126. [PubMed: 3541536]

Gahl WA, Dalakas MC, Charnas L, Chen KT, Pezeshkpour GH, Kuwabara T, Davis SL, Chesney RW, Fink J, Hutchison HT. Myopathy and cystine storage in muscles in a patient with nephropathic cystinosis. New England Journal of Medicine. 1988; 319:1461–1464. [PubMed: 3185663]

Gahl WA, Thoene JG, Schneider JA. Cystinosis. New England Journal of Medicine. 2002; 347:111–121. [PubMed: 12110740]

Gieselmann V, Polten A, Kreysing J, von Figura K. Molecular genetics of metachromatic leukodystrophy. Journal of Inherited Metabolic Disesase. 1994; 17:500–509.

Jonas AJ, Conley SB, Marshall R, Johnson RA, Marks M, Rosenberg H. Nephropathic cystinosis with central nervous system involvement. The American Journal of Medicine. 1987; 83:966–970. [PubMed: 3674101]

Just MA, Carpenter PA, Maguire M, Diwadkar V, McMains S. Mental rotation of objects retrieved from memory: a functional MRI study of spatial processing. Journal of Experimental Psychology: General. 2001; 130:493–504. [PubMed: 11561923]

Kates WR, Warsofsky IS, Patwardhan A, Abrams MT, Liu AM, Naidu S, Kaufmann WE, Reiss AL. Automated Talairach atlas-based parcellation and measurement of cerebral lobes in children. Psychiatry Research. 1999; 91:11–30. [PubMed: 10496689]

Kessler A, Biasibetti M, Feksa LR, Rech VC, da Silva Melo DA, Wajner M, Dutra-Filho CS, de Souza Wyse AT, Wannmacher CM. Effects of cysteamine on oxidative status in cerebral cortex of rats. Metabolic Brain Disease. 2007

Kim JJ, Crespo-Facorro B, Andreasen NC, O'Leary DS, Zhang B, Harris G, Magnotta VA. An MRI-based parcellation method for the temporal lobe. Neuroimage. 2000; 11:271–288. [PubMed: 10725184]

Kleta R, Gahl WA. Pharmacological treatment of nephropathic cystinosis with cysteamine. Expert Opinion Pharmacotherapy. 2004; 5:2255–2262.

Klingberg T, Forssberg H, Westerberg H. Increased brain activity in frontal and parietal cortex underlies the development of visuospatial working memory capacity during childhood. Journal of Cognitive Neuroscience. 2002; 14:1–10. [PubMed: 11798382]

Le Bihan D, Mangin JF, Poupon C, Clark CA, Pappata S, Molko N, Chabriat H. Diffusion tensor imaging: concepts and applications. Journal of Magnetic Resonance Imaging. 2001; 13:534–546. [PubMed: 11276097]

Levine S, Paparo G. Brain lesions in a case of cystinosis. Acta Neuropathologica (Berl). 1982; 57:217–220. [PubMed: 7124349]

Maurice T, Hippert C, Serratrice N, Dubois G, Jacquet C, Antignac C, Kremer EJ, Kalatzis V. Cystine accumulation in the CNS results in severe age-related memory deficits. Neurobiology of Aging. 2007

McGrew, KS.; Woodcock, RW. Woodcock-Johnson Psychoeducational Battery and Scales of Independent Behavior: Subtest Norms for the WJ/SIB Assessment System. DLM Teaching Resources; U.S.A.: 1985.

Moritani, T.; Ekholm, S.; Westesson, P. Diffusion-weighted MR imaging of the brain. Springer; Berlin: 2004.

Mukherjee P, Miller JH, Shimony JS, Conturo TE, Lee BC, Almli CR, McKinstry RC. Normal brain maturation during childhood: developmental trends characterized with diffusion-tensor MR imaging. Radiology. 2001; 221:349–358. [PubMed: 11687675]

Mukherjee P, Miller JH, Shimony JS, Philip JV, Nehra D, Snyder AZ, Conturo TE, Neil JJ, McKinstry RC. Diffusion-tensor MR imaging of gray and white matter development during normal human brain maturation. American Journal of Neuroradiology. 2002; 23:1445–1456. [PubMed: 12372731]

Nichols SL, Press GA, Schneider JA, Trauner DA. Cortical atrophy and cognitive performance in infantile nephropathic cystinosis. Pediatric Neurology. 1990; 6:379–381. [PubMed: 2073300]

Oliver RT, Thompson-Schill SL. Dorsal stream activation during retrieval of object size and shape. Cognitive, Affective, and Behavioral Neuroscience. 2003; 3:309–322.

Pierpaoli C, Jezzard P, Basser PJ, Barnett A, Di Chiro G. Diffusion tensor MR imaging of the human brain. Radiology. 1996; 201:637–648. [PubMed: 8939209]

Pins D, Meyer ME, Foucher J, Humphreys G, Boucart M. Neural correlates of implicit object identification. Neuropsychologia. 2004; 42:1247–1259. [PubMed: 15178176]

Rao H, Zhou T, Zhuo Y, Fan S, Chen L. Spatiotemporal activation of the two visual pathways in form discrimination and spatial location: a brain mapping study. Human Brain Mapping. 2003; 18:79–89. [PubMed: 12518288]

Ross DL, Strife CF, Towbin R, Bove KE. Nonabsorptive hydrocephalus associated with nephropathic cystinosis. Neurology. 1982; 32:1330–1334. [PubMed: 6890639]

Scarvie KM, Ballantyne AO, Trauner DA. Visuomotor performance in children with infantile nephropathic cystinosis. Perceptual Motor Skills. 1996; 82:67–75.

Schmithorst VJ, Holland SK, Dardzinski BJ. Developmental differences in white matter architecture between boys and girls. Human Brain Mapping. 2007a

Schmithorst VJ, Holland SK, Plante E. Object identification and lexical/semantic access in children: a functional magnetic resonance imaging study of word-picture matching. Human Brain Mapping. 2007b; 28:1060–1074. [PubMed: 17133401]

Schmithorst VJ, Wilke M, Dardzinski BJ, Holland SK. Cognitive functions correlate with white matter architecture in a normal pediatric population: A diffusion tensor MRI study. Human Brain Mapping. 2005

Schmithorst VJ, Wilke M, Dardzinski BJ, Holland SK. Correlation of white matter diffusivity and anisotropy with age during childhood and adolescence: a cross-sectional diffusion-tensor MR imaging study. Radiology. 2002; 222:212–218. [PubMed: 11756728]

Schneider JF, Il'yasov KA, Hennig J, Martin E. Fast quantitative diffusion-tensor imaging of cerebral white matter from the neonatal period to adolescence. Neuroradiology. 2004; 46:258–266. [PubMed: 14999435]

Shen L, Hu X, Yacoub E, Ugurbil K. Neural correlates of visual form and visual spatial processing. Human Brain Mapping. 1999; 8:60–71. [PubMed: 10432182]

Smith M, Furlong CE, Greene AA, Schneider JA. Cystine: binding protein assay. Methods in Enzymology. 1987; 143:144–148. [PubMed: 3309549]

Smolin LA, Clark KF, Schneider JA. An improved method for heterozygote detection of cystinosis, using polymorphonuclear leukocytes. American Journal of Human Genetics. 1987; 41:266–275. [PubMed: 3618595]

Snook L, Paulson LA, Roy D, Phillips L, Beaulieu C. Diffusion tensor imaging of neurodevelopment in children and young adults. Neuroimage. 2005; 26:1164–1173. [PubMed: 15961051]

Stejskal EO, Tanner JE. Spin diffusion measurements: spin echoes in the presence of a time-dependent field gradient. Journal of Chemical Physics. 1965; 42

Stiles, J. Spatial cognitive development following prenatal or perinatal focal brain injury. In: Levin, H.; Grafman, J., editors. Cerebral reorganization of function after brain damage. Oxford; New York: 2000. p. 201-217.

Thomas KM, King SW, Franzen PL, Welsh TF, Berkowitz AL, Noll DC, Birmaher V, Casey BJ. A developmental functional MRI study of spatial working memory. Neuroimage. 1999; 10:327–338. [PubMed: 10458945]

Trauner D, Chase C, Scheller J, Katz B, Schneider JA. Neurologic and cognitive deficits in children with cystinosis. Journal of Pediatrics. 1988; 112:912–914. [PubMed: 3373397]

Trauner DA, Spilkin AM, Williams J, Babchuck L. Specific cognitive deficits in young children with cystinosis: evidence for an early effect of the cystinosin gene on neural function. Journal of Pediatrics. 2007; 151:192–196. [PubMed: 17643777]

Ungerleider, L.; Mishkin, M. Two cortical visual systems. In: Ingle, D.; Goodale, MA.; Mans, RJW., editors. Analysis of visual behavior. MIT Press; Cambridge, MA: 1982. p. 549-586.

Ungerleider LG, Haxby JV. `What' and `where' in the human brain. Current Opinion in Neurobiology. 1994; 4:157–165. [PubMed: 8038571]

van der Knaap MS, Breiter SN, Naidu S, Hart AA, Valk J. Defining and categorizing leukoencephalopathies of unknown origin: MR imaging approach. Radiology. 1999; 213:121–133. [PubMed: 10540652]

Vogel DG, Malekzadeh MH, Cornford ME, Schneider JA, Shields WD, Vinters HV. Central nervous system involvement in nephropathic cystinosis. Journal of Neuropathology and Experimental Neurology. 1990; 49:591–599. [PubMed: 2230837]

Wechsler, D. Wechsler Intelligence Scale for Children-III. Psychological Corporation; San Antonio, TX: 1991.

Wechsler, D. Wechsler Preschool and Primary Scale of Intelligence-Revised. Psychological Corporation; San Antonio, TX: 1989.

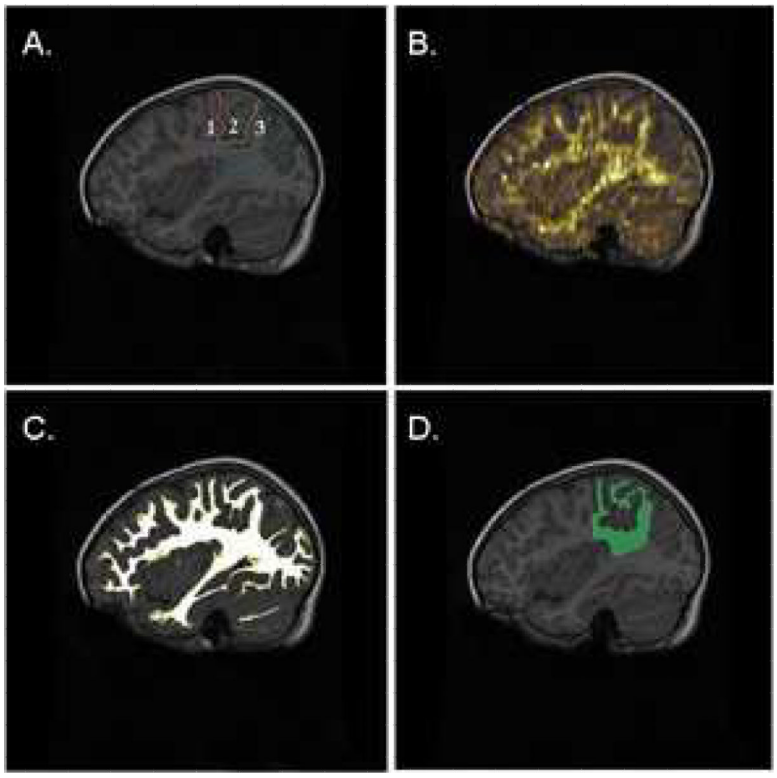


**Figure 1.**

(A) Representative examples of region of interest (ROI) definition of the parietal lobe with its subdivisions on a T1-weighted anatomical image in a control participant; (B) Overlay of the fractional anisotropy map on anatomical image; (C) Illustration of segmented white matter mask used for extracting mean diffusion parameters from ROIs; (D) Product of white matter segment and parietal ROI.

Note. Age of control participant is 5.5 years. Anterior-posterior outline of regions is: postcentral gyrus (purple-orange); superior parietal lobule (orange-green); inferior parietal lobule (green-blue).

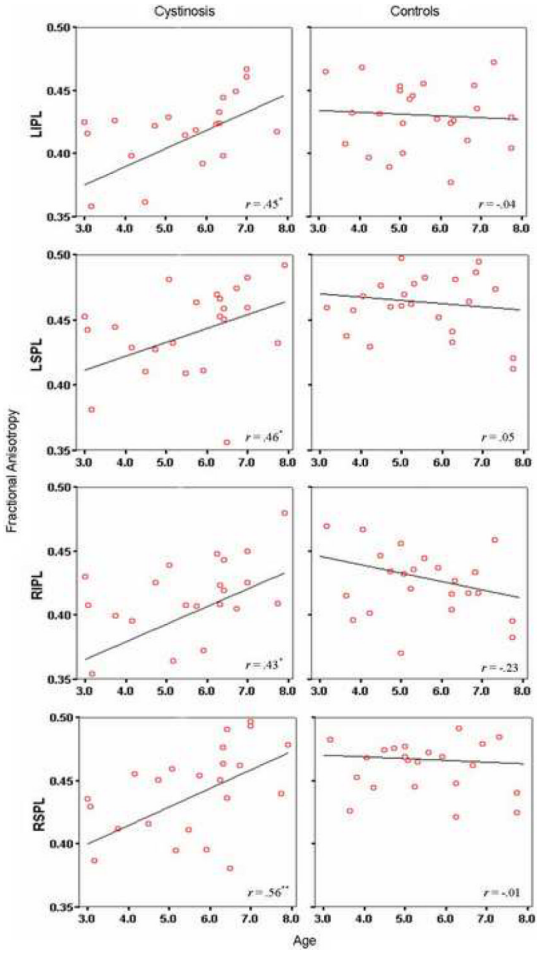


**Figure 2.**

Bivariate scatterplots depicting the relationship between age and fractional anisotropy in cystinosis and control participants.

*$p$<.05

**$p$<.01

Abbreviations. LIPL = left inferior parietal lobule; LSPL = left superior parietal lobule; RIPL = right inferior parietal lobule; RSPL = right superior parietal lobule.

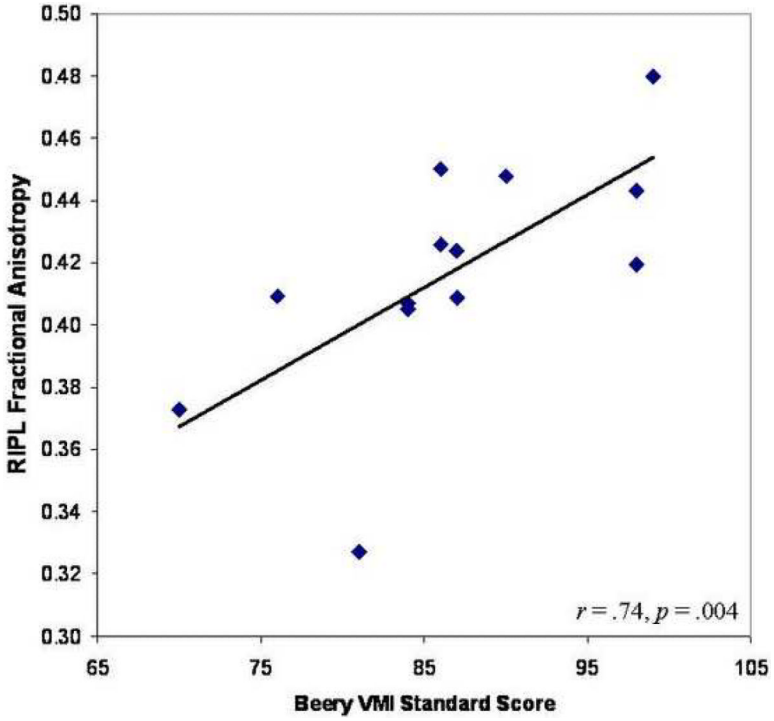


**Figure 3.**
Bivariate relationship between fractional anisotropy in the right inferior parietal lobule (RIPL) and Beery Visual-Motor Integration (VMI) performance in school-age cystinosis participants.

## Table 1

Behavioral performance in cystinosis children and controls

| | Cystinosis Mean ± SD *(n = 24)* | Controls Mean ± SD *(n = 24)* | T | P |
|---|---|---|---|---|
| Spatial Relations Test | 103 ± 10.8 | 116 ± 8.5 | 4.6 | .008 * |
| Visual-Motor Integration Test | 89 ± 12.0 | 107 ± 15.9 | 4.0 | .001 * |
| Performance IQ | 90 ± 12.0 | 112 ± 12.0 | 6.0 | <.001 * |
| Verbal IQ | 95 ± 12.2 | 113 ± 14.8 | 4.6 | <.001 * |

* Significant at $p < .05$, reported p-values are adjusted using the Hochberg correction for multiple comparisons

**Table 2**

Fractional anisotropy and mean diffusivity in parietal and temporal regions in cystinosis children and controls

| | Fractional Anisotropy | | | | Mean Diffusivity | | | |
|---|---|---|---|---|---|---|---|---|
| | **Cystinosis Mean ± SD *(n = 24)*** | **Controls Mean ± SD *(n = 24)*** | **F** | **P** | **Cystinosis Mean ± SD *(n = 24)*** | **Controls Mean ± SD *(n = 24)*** | **F** | **P** |
| LIPL | .41 ± .04 | .43 ± .03 | 3.23 | .08 | .74 ± .08 | .70 ± .04 | 2.97 | .09 |
| LSPL | .44 ± .04 | .46 ± .03 | 6.98 | .01* | .74 ± .08 | .69 ± .03 | 3.95 | .04* |
| RIPL | .40 ± .05 | .43 ± .03 | 5.71 | .02* | .73 ± .07 | .70 ± .04 | 2.56 | .12 |
| RSPL | .44 ± .04 | .47 ± .03 | 7.97 | .01* | .75 ± .08 | .70 ± .04 | 4.62 | .04* |
| LITG | .38 ± .05 | .38 ± .04 | 0.52 | .48 | .72 ± .04 | .72 ± .03 | 0.22 | .64 |
| RITG | .37 ± .05 | .36 ± .04 | 0.02 | .89 | .72 ± .03 | .71 ± .05 | 1.10 | .30 |

Abbreviations. L = Left; R = Right; IPL = inferior parietal lobule; SPL = superior parietal lobule; ITG = inferior temporal gyrus

*Significant at $p < .05$, reported $p$-values are adjusted using the Hochberg correction for multiple comparisons